Flexible Paper-Based Polyacrylic Acid-Coated Silver Nanoparticle Film Sensors Prepared by Inkjet Printing for Efficient Ammonia Detection at Room Temperature

Mingyue Peng
Ningbo University
Dawu Lv
Ningbo Institute of Materials Technology and Engineering Chinese Academy of Sciences: Ningbo Institute of Industrial Technology Chinese Academy of Sciences
Wenfeng Shen
Ningbo Institute of Materials Technology and Engineering Chinese Academy of Sciences: Ningbo Institute of Industrial Technology Chinese Academy of Sciences
Weijie Song
Ningbo Institute of Materials Technology and Engineering Chinese Academy of Sciences: Ningbo Institute of Industrial Technology Chinese Academy of Sciences
Ruiqin Tan (tanruiqin@nbu.edu.cn)
Ningbo University https://orcid.org/0000-0003-3743-4884

Original Research

Keywords: paper-based film sensor, polyacrylic acid, silver nanoparticles, ammonia sensor, inkjet printing

Posted Date: February 4th, 2021

DOI: https://doi.org/10.21203/rs.3.rs-173204/v1

Abstract

A series of disposable gas-sensing paper-based film sensors were prepared rapidly by inkjet printing polyacrylic acid-coated silver nanoparticle (PAA/AgNP) ink onto the ordinary copy paper. The surface morphologies and chemical structures of the printed PAA/AgNP based sensing films with various thicknesses and spacing widths of interdigital electrodes were characterized. The electrical properties and the gas sensing performance of the film sensors were investigated and the results showed that the PAA/AgNP film sensors presented excellent selectivity, reproducibility and long-term stability to ammonia (NH_3) gas at room temperature. The response of the PAA/AgNP film sensor to NH_3 with the concentration of 25 ppm is 42.6% at 20℃ and 50% relative humidity (RH). The influences of thickness, spacing of interdigital electrodes and relative humidity on the sensing properties of the PAA/AgNP film sensors were also discussed and analyzed. Additionally, the PAA/AgNP film sensor presented perfect flexible stability and showed minor change in response value after 100 folding/extending cycles with the angle of 90°. In conclusion, the proposed high-performance paper based PAA/AgNP thin film sensor holds great promise for flexible, low-cost, portable, disposable and recyclable application in detecting NH_3 at room temperature.

1. Introduction

Ammonia (NH_3) has been widely employed in many industries like food processing, medical prognosis, agriculture, and refrigeration systems [1]. However, excessive NH_3 emission not only does harm to the surrounding environment and ecosystem, but also has negative impact on human's health [2]. NH_3 with a concentration higher than 35 ppm will carry a risk to damage the human cells, irritate skin and eyes, and destroy the mucosa of respiratory tract within 15 minutes [3]. Accordingly, it is greatly demanded to develop highly sensitive, disposable, convenient, and economical devices for NH_3 detection at room temperature. There are many methods to detect NH_3, including mass spectrometry, chemical analysis, infrared spectrophotometry, gas chromatography, and gas sensor [4] up to now, among which, the gas sensor is the most commonly used for NH_3 detection due to its simplicity and convenience [5].

Printing technology is aiding and revolutionizing the booming field of flexible electronic devices by providing a cost-effective way for processing kinds of electronic materials which are compatible with low-cost and flexible substrates [6]. Recently, inkjet printing has received much attention in material and sensor preparation procedures due to its unique advantages, such as the potential for non-vacuum and low temperature processing, low materials waste, easy control, etc. [7]. What is more, inkjet printing technology is environmentally friendly because it does not need any harmful chemicals to wash away the excess materials on the substrate surface [8]. Meanwhile its advantages of fast fabrication and ease of mass production can help lower the cost of the inkjet-printed devices [9].

Selecting optimal substrates is one of important matters to effectively realize low-cost and flexible inkjet-printed devices [10]. Paper, made of plant fibers, is one of the cheapest materials in the world. It has the

advantages of availability, flexibility, disposability and recyclability. In addition, paper allows passive liquid transport and has excellent compatibility with chemicals [9, 11]. Moreover, paper has inherent porous structure and rough surface, which can provide a large surface area compared with flat glass or nonporous plastic [12]. These advantages make paper a conducive platform for ink-jet printing to develop flexible and low-cost functional devices [13]. Up to now a few paper-based NH_3 sensors have been presented in the literatures. Avisek Maity et al. [14] reported a type of paper sensor working at room temperature can be made using perovskite halide $CH_3NH_3PbI_3$ (MAPI) to detect the presence of NH_3 by color change. However, MAPI has strong toxicity, which is not environmentally friendly and is not suitable for daily NH_3 detection. Lianghui Huang et al. [15] fabricated colorimetric NH_3 gas sensors by facile filtration of modified Berthelot's reagents on a porous paper substrate for the chemical analysis of wastewater or seawater. However, this detection was based on the separation of NH_3 gas from the aqueous matrix and irreversible chemical reactions at the gas-solid interface, which may be not gainful for NH_3 detection in air.

In this work, we first report the preparation of high performance polyacrylic acid-coated silver nanoparticle (PAA/AgNP) based NH_3 sensor on paper substrate by inkjet printing at room temperature. PAA/AgNP based gas sensing films with different thicknesses were fabricated by printing inks onto the paper substrate coated with interdigital silver electrodes of different interdigital spacing. The electrical response of PAA/AgNP thin films towards NH_3 with low concentration (1–25 ppm) was demonstrated at room temperature and the gas sensing mechanism was proposed.

2. Experimental

2.1 Materials

All chemicals used in this work were analytical grade reagents without further purification. Triethanolamine (TEA, ≥ 99.0%), polyacrylic acid (PAA, average M. W. 5000, 50 wt.% solution in H_2O) and $AgNO_3$ were purchased from Sinopharm Chemical Reagent Co., Ltd. Sodium dodecyl sulfate (SDS) was purchased from Aladdin, China. Deionized water was used in all of the experiments. The standard dry gas of 50 ppm NH_3, using high pressure air as the equilibrium gas, was purchased from Zhengzhou Xingdao Chemical Technology Co., Ltd. While the sample gases of formaldehyde, methanol and ethanol are obtained by the corresponding static liquid vapors. The calculation of the concentration is shown in **Eq. (1)**:

$$V_L=P*C_{ppm}*V_C*M/(R*T*\rho*\omega) \quad (1)$$

where V_L is the volume of corresponding organic liquid, P is the gas pressure, C_{ppm} is the gas concentration, V_C is the volume of test cavity, R is the gas constant, T is the temperature and ω, ρ and M are the mass fraction, the density and the molar mass of the organic liquid respectively. According to the actual situation of the static test in this experiment, the gas pressure P is $1.01*10^5$ Pa, R is 8.314, T is

273.15 K, and the volume of the quartz testing tube is 50 ml. Taking pure ethanol gas as an example, M is 46 g/mol, ρ is 0.791 g/ml and ω is 1.

2.2 Fabrication of PAA/AgNP ink and thin film sensor

Based on our previous work [16], we made some improvements in preparing AgNPs in order to implement the fabrication of PAA/AgNP film sensor. The procedure to synthesize precursor ink is shown in Fig. 1. Firstly, TEA (15 g) and PAA (4 g) were dissolved in deionized water (60 ml). This mixture was stirred at room temperature for 2 h, resulting in a transparent colloidal solution. Secondly, $AgNO_3$ (9 g) was dissolved in 10 ml of deionized water and underwent ultrasonic dispersion for 20 minutes, which then was dropped into the transparent colloidal solution with a dropper. Thirdly, this mixture of TEA, PAA and $AgNO_3$ was stirred at room temperature for 18 h and then heated to 65℃ with continuous stirring for 2 h, leading to the PAA/AgNP solution with the color of dark red. The PAA/AgNP ink was prepared by mixing PAA/AgNP aqueous solution and SDS with the mass ratio of 1:0.009. Here, SDS used as surfactant to decrease the surface tension of the ink. Finally, the PAA/AgNP ink was loaded into different cartridges and then printed onto a paper substrate coated with interdigital silver electrodes using our modified ink-jet printer. The details are shown in Fig. 1a. After printing, the films were dried in air for 2 h. As shown in Fig. 1b, the PAA/AgNP film sensors were divided into four types according to the spacing between the neighboring interdigitated electrode fingers. One had no electrode fingers, and the spacing widths of other three were 5.0 mm, 2.0 mm and 1.0 mm, marked as E-1, E-2, E-3 and E-4, respectively.

2.3 Characterization of PAA/AgNP thin films

The surface morphologies of the samples were examined by a field emission scanning electron microscope (FESEM, Hitachi S4800). The Energy-dispersive X-ray spectroscopy (EDX) was used in order to analyze the composition of the PAA/AgNP film sensor. The thermogravimetric differential thermal analysis (TG/DTA) of the PAA/AgNP powder was performed using a Perkin-Elmer Pyris Diamond TG/DTA in air with a heating rate of 10 K min^{-1}. The chemical structure and bonding characteristics were investigated by Fourier transform infrared (FTIR) spectroscopy (Model: Perkin Elmer100). X-ray photoelectron spectroscopy (XPS) was performed in a Thermo Scientific K-Alpha X-ray photoelectron spectrometer, using monochromatic Al Kα radiation (1486.6 eV). The XPS spectra were calibrated with reference to the C 1s speak (284.8 eV).

The detailed gas-sensing experimental process and platform have been shown in Fig. 2. Sensing measurements were performed in a quartz tube with a volume of 50 ml. Standard NH_3 (Zhengzhou Xingdao Chemical Technology Co., Ltd.) was firstly filled into a gas sampling bag (50 ml, Dalian Delin Gas Packing Co., Ltd., China), and then was injected into the quartz testing tube through the syringe to obtain the NH_3 with corresponding diluted concentration. The resistances of the films were measured by a digital multimeter (VICTOR 8246A), and the values were recorded (every 0.3 s) by the matching LabVIEW program. The experimental relative humidity was about 50% at 20℃. The effect of different humidity on the response of the sensor was examined at 20℃ using a humidity meter purchased from Shanghai Duohe Equipment Co., Ltd, which could control the testing temperature and humidity precisely.

At a certain temperature and humidity, the sensor response (S) was defined as $S= (R-R_0)/ R_0 \times 100$ (%), where R_0 and R represent the resistance values of the sensor in air and tested gases, respectively. The response time is defined as the time required for the resistance variation value to reach 90% of the maximum value. The recovery time is defined as the time required for the resistance recovery value to reach 10% of the maximum value after the gas was discharged.

3. Results And Discussion

3.1 Microstructure of PAA/AgNP thin film

The surface and cross-section morphology of the PAA/AgNP sensing film of E-4 printed for 20 cycles was characterized by FESEM. The interdigital electrode of the white part and the printed film layer of the black part are clearly observed in Fig. 3a. The thickness of the paper is about 42.4 μm, while the Ag electrode has a thickness of approximately 30.3 μm as shown in the cross-section of PAA/AgNP film in Fig. 3b. Figure 3c shows a partial enlarged view of the printing layer in Fig. 3b. AgNPs with an average size of 135 nm accumulate on the surface, which can well penetrate into the paper and attached to the fiber due to the porous structure of the substrate. The EDX result shows the presence of Ag from AgNPs and C from PAA can clearly be identified.

The TG/DTA result of the PAA/AgNP composite is presented in Fig. 4. The sample shows a continuous weight loss from room temperature to 950℃ with a cumulative weight loss of 13.4%, which is attributed to the desorption of the organic constituents from the surface of the AgNPs [16]. There is a strong endothermic peak at approximately 955℃, which may be attributed to the melting of bulk silver. There is a cumulative loss of 0.3% from 955℃ to 1010℃, which may be attributed to the temperature disturbance. These results demonstrate that the solid AgNPs powder contained more than 86.3 wt% silver.

The FTIR absorption spectrum of the PAA/AgNP film is illustrated in **Fig. 5**. The peak at 1700 cm^{-1} is assigned to C = O stretching vibration mode, and the wide peak at 3300 cm^{-1} corresponds to O-H stretching mode [17]. This result suggests that the film contains carboxyl group which origins from PAA.

Figure 6 shows the XPS spectra for Ag 3d peaks of pure AgNPs and PAA/AgNP sensing film, respectively. Based on the results of deconvolution, the AgNPs exhibit two characteristic peaks at binding energies of 374.2 eV (Ag $3d_{3/2}$) and 368.2 eV (Ag $3d_{5/2}$), corresponding to metallic Ag. However, the PAA/AgNP sensing film shows the presence of two Ag 3d chemical states as one doublet at 374.0 eV (Ag $3d_{3/2}$) and 368.0 eV (Ag $3d_{5/2}$), and the other one at 376.0 eV (Ag $3d_{3/2}$) and 370.0 eV (Ag $3d_{5/2}$). The shifting of the doublet to higher binding energy may be attributed to the interfacial interaction and charge transferring between the AgNP and the polymer (PAA) [18].

3.2 Electrical property of PAA/AgNP thin film

The thickness of the PAA/AgNP film could be controlled by the number of printing cycles. The resistance curves of the films with different printing cycles and different shapes of interdigital electrodes are shown in Fig. 7. It illustrates the changes in resistances of the PAA/AgNP thin films associated with different spacing of interdigital silver electrodes and number of printing cycles. At the beginning, the resistances of E-1, E-2 and E-3 were all larger than 50 MΩ with the printing cycles less than 5, which was beyond the range of the multimeter. Increasing the number of printing cycles leads to an increase in the film's thickness and a decrease in the film's resistance. The high resistance of the films printed for 5 cycles may be due to the discontinuity of the film surface. The films become more continuous and their resistances decrease obviously after printed for 9 cycles. Afterwards the resistances reduce slightly and then tend to be stable. For the same printing cycle, the resistances of PAA/AgNP thin films reduce as the spacing between interdigital electrode fingers decreases. This may be determined by the length of the conductive path in PAA/AgNP layer between two interdigital electrode fingers [19]. So in the next study, we chose the sensor of E-4 printed for 9 cycles with low initial resistance for the performance investigation.

3.3 NH_3-sensing performance

3.3.1 The selectivity of PAA/AgNP film sensor

Selectivity is the most critical parameter for gas sensor, which determines whether the sensor could be used in complex atmospheric environment [20]. Herein, three kinds of interfering gases including 1000 ppm formaldehyde, 100 ppm methanol and ethanol were chosen to evaluate the selectivity of the PAA/AgNP film sensor (E-4, printed for 9 cycles) to NH_3 at 20℃. As shown in Fig. 8, the PAA/AgNP film sensor exhibits a significant response of 42.6% to 25 ppm NH_3, while it shows low responses of -10.2% and − 5.8% to methanol and ethanol with concentrations 4 times higher than NH_3, and little response of -1.7% to formaldehyde with a concentration 40 times higher than NH_3. What is more, the PAA/AgNP film sensor responds with a decrease in resistance when exposed in formaldehyde, methanol and ethanol, which is contrary to its response to NH_3. It is confirmed that the PAA/AgNP film sensor possesses a better selectivity to NH_3 and is a promising candidate for future applications to detect NH_3 at room temperature.

3.3.2 The response of PAA/AgNP film sensor to NH_3 with various concentrations

The real-time response-recovery curve of the PAA/AgNP film sensor (E-4, printed for 9 cycles) for 1–25 ppm NH_3 at 20℃ is shown in Fig. 9, which exhibits excellent dynamic response/recovery characteristics to NH_3 gas. The response value of the PAA/AgNP film sensor is 1.6% to NH_3 with the minimum concentration of 1 ppm. The response value increases with the concentration of NH_3 rising, which reaches to 42.6% when the NH_3 concentration is 25 ppm. It is inferred that there is a linear relationship between the response value and the NH_3 concentration in the inset of Fig. 9. As presented in Fig. 10, the PAA/AgNP film sensor (E-4, printed for 9 cycles) responds quickly and the response time is about 52 s with an increase in resistance when exposed to NH_3. The resistance falls back to the initial state within a

short time and the recovery time is 231 s, without baseline drift after it is placed in air, which reveals a good reversibility of the PAA/AgNP film sensor.

3.3.3 The stability of PAA/AgNP film sensor

Stability is one of the main evaluation criteria for gas sensors and also a comprehensive performance of sensor reliability in applications. In terms of the length of time, it is usually divided into short-term repeatability and long-term stability [21].

In order to investigate the stability of PAA/AgNP film sensor, we have tested short-term repeatability and long-term stability of the E-4 sensor printed for 9 cycles. Figure 11a illustrates a series of real-time response of PAA/AgNP film sensor to 25 ppm NH_3 at 20℃. It is observed that the sensor could be continuously operated for five cycles with similar response values, and the response could fully return to the initial state at the end of each response-recovery cycle, which indicates the PAA/AgNP film sensor can be reproduced. The long-term stability of the PAA/AgNP film sensor aged for a month was tested to 25 ppm NH_3 at 20℃ and the result has been shown in Fig. 11b. It is found that the responses of the film keep similar and stable as the values a month before. These results indicate a remarkable short-term repeatability and long-term stability of the PAA/AgNP thin film sensor.

3.3.4 The influence of printing cycles and different spacing of interdigital electrodes on the response of PAA/AgNP film sensor

The thickness of the films is an important factor that influences the sensor response. Via utilizing the ink-jet printing method, the thickness of the films could be easily changed by varying the number of printing cycles [22]. Figure 12a illustrates real-time response curves of PAA/AgNP sensor to 25 ppm NH_3 at different printing cycles. As shown in Fig. 12b, it is evident that the responses of the E-4 film sensors increase initially with the increasing of printing cycles. When the number of printing cycles are 5, 9 and 11, the responses of the films to 25 ppm NH_3 are 39.5%, 42.6% and 51.1%, respectively. The optimal response is obtained after printed for 13 cycles with the response value of 66.5%. However, further increasing the printing cycles leads to a decrease of the sensor response. When the films are printed for 15 and 20 cycles, the responses are 58.5% and 49.2%, respectively. The above results indicate that the sensor response is largely dependent on the film's thickness. Both too thin (printing for 5 cycles) and too thick (printing for 20 cycles) films will lead to limit the NH_3 adsorption capacity.

In order to investigate the NH_3 sensing properties of the PAA/AgNP film sensor with different spacing of fingers to 25 ppm NH_3 at 20℃, the responses of four type sensors printed for 9 cycles are shown in Fig. 13. The inset figure of Fig. 13 are the dynamic response curves of the sensors. The responses of E-1, E-2, E-3 and E-4 are 127.6%, 85.3%, 68.1% and 42.6%, respectively. It is clear to find that the greater spacing between the fingers of the PAA/AgNP film sensors, the higher response to NH_3. According to C. M. Yang [19], it is concluded that the sensor with a larger spacing of interdigital electrodes has a higher surface area ratio (the ratio of the paper surface area to the unit area including the paper and Ag

electrode, i.e. paper area / (paper area + Ag area)), which insures more NH_3 could be adsorbed for a higher response.

3.3.5 The influence of humidity on the response of PAA/AgNP film sensor

Relative humidity is one of the major matters which could affect the gas sensing performance of PAA/AgNP film sensor. The influence of relative humidity on the NH_3-sensing performance of PAA/AgNP film sensor (E-4, printed for 9 cycles) was examined by detecting the response to 25 ppm NH_3 under various relative humidity as shown in Fig. 14. The responses of PAA/AgNP film sensor are 124.5%, 76.4%, 42.6%, 35.8% and 26.3% under relative humidity of 30%, 40%, 50%, 60% and 70%, respectively. It is observed that the sensor response decreases with increasing the relative humidity. It is suggested that water molecules occupy some of the active sites on the surface of flexible sensor and hinder the adsorption of target gas molecules at a higher humidity, which is the probable cause to the decreasing of the response at higher humidity conditions [23, 24]. From Fig. 14, it is shown that the sensor's response is greatly affected by the relative humidity. Based on this, improving the sensor’s anti-interference to humidity is the direction of our future work. Adding a humidifier to the test instrument to fix the humidity in the quartz testing tube at a constant value is also an optional proposal to eliminate the influence of humidity on the sensor’s performance.

3.3.6 Flexibility of PAA/AgNP film sensor

The sensing properties of PAA/AgNP film sensor (E-4, printed for 9 cycles) to different concentrations of NH_3 was evaluated after 100 folding/extending cycles with the folding angle of 90°, and the results are shown in Fig. 15. After 100 folding/extending cycles, no obvious response change of the sensor is observed for 1 ppm and 25 ppm NH_3. A slight response increases with a standard deviation of less than 2% could be seen for 5 ppm, 10 ppm and 15 ppm NH_3. The inset of Fig. 15 illustrates the response-recovery curves of PAA/AgNP film sensor to 25 ppm NH_3, which reveals no obvious response change for the sensor after 100 folding/extending cycles. All the results prove that the PAA/AgNP film sensor possesses a great flexibility for sensing properties, which is promising to be integrated into hand-held or wearable device.

3.4 Sensing mechanism

The sensing mechanism of the excellent response to NH_3 by PAA/AgNP film sensor is proposed and illustrated in Fig. 16. As the XPS results inferred, there exists a charge transferring between the silver particles and the PAA coating [18]. When the PAA/AgNP film sensor is placed in air (Fig. 16a), the electrons of AgNPs normally transport through the AgNPs to the interface between AgNPs and PAA and attract H^+ of the PAA. Due to the fact that the AgNPs are coated by PAA, the transport of H^+ between PAA and AgNPs becomes weak, which results in the resistance of the sensor being relatively large. When the PAA/AgNP film sensor is exposed in NH_3 (Fig. 16b), the NH_3 molecule attracts the H^+ of PAA to form

NH_4^+, which leads to the interfacial electrons between AgNPs and PAA flowing back into the AgNPs. As a result, the conductive paths reduced resulting in the increase in the resistance of the PAA/AgNP film sensor. On the contrary, when the sensor is exposed in ethanol, methanol and formaldehyde, their molecules will give H^+ to PAA, which promotes electrons flowing to the interfacial between AgNPs and PAA. As a result, the conductive paths increased resulting in the decrease in the resistance of the PAA/AgNP film sensor. However, compared with methanol and ethanol, formaldehyde has a poor ability to give H^+, so the sensor shows almost no response to 1000 ppm formaldehyde.

Conclusions

In this work, a flexible room temperature NH_3 sensor based on PAA/AgNP films with different thickness and spacing of interdigital electrodes on paper substrates were successfully developed by inkjet printing method. The NH_3-sensing performance was evaluated and the results demonstrated that the PAA/AgNP film sensor possessed remarkable selectivity, response, reproducibility, long-term stability, low detection limit (1 ppm) and outstanding flexibility. Meanwhile the inkjet printing technology using paper substrate help to improve the processing of low-cost, portable, disposable, recyclable film sensors.

Declarations

Credit authorship contribution statement

Mingyue Peng: Investigation, Methodology, Writing - original draft Data curation. Dawu Lv: Conceptualization, Doing auxiliary work. Wenfeng Shen: Writing - review & editing, Supervision. Weijie Song: Funding acquisition, Project administration. Ruiqin Tan: Supervision.

Declaration of Competing Interest

The authors declare that they have no known competing financial interests or personal relationships that could have appeared to influence the work reported in this paper.

Acknowledgements

This work was financially supported by Zhejiang Provincial Natural Science Foundation of China (LGG21F040001) and K.C. Wong Magna Fund in Ningbo University. Author 1 and Author 2 contributed equally to this work.

References

[1] C. Zhu, U. Cakmak, O. Sheikhnejad, X. Cheng, X. Zhang, Y. Xu, S. Gao, H. Zhao, L. Huo, Z. Major, Nanotechnology 30, 255502 (2019).

[2] Y. Xiong, H. Li, X. Li, T. Guo, L. Zhu, Q. Xue, Nanotechnology 30, 135501 (2019).

[3] T. Mérian, N. Redon, Z. Zujovic, D. Stanisavljev, J. L. Wojkiewicz, M. Gizdavic-Nikolaidis, Sensor Actuat. B-Chem 203, 626 (2014).

[4] K. Mistewicz, M. Nowak, D. Stroz, A. Guiseppi-Elie, Talanta 189, 225 (2018).

[5] D. Lv, W. Chen, W. Shen, M. Peng, X. Zhang, R. Wang, L Xu, W. Xu, W. Song, R. Tan, Sensor Actuat B-Chem 298, 126890 (2019).

[6] S. Khan, L. Lorenzelli, R. S. Dahiya, IEEE Sens. J 15, 3164 (2015).

[7] Y. S. Rim, S. H. Bae, H. Chen, N. De Marco, Y. Yang, Adv. Mater 28, 4415 (2016).

[8] F. Loffredo, A. D. G. D. Mauro, G. Burrasca, V. La Ferrara, L. Quercia, E. Massera, G. D. Francia, D. D. Sala, Sensor Actuat B-Chem 143, 421 (2009).

[9] P. K. Sekhar, J. S. Kysar, J. Electrochem. Soc 164, B113 (2017).

[10] S. Kim, B. Cook, T. Le, J. Cooper, H. Lee, V. Lakafosis, R. Vyas, R. Moro, M. Bozzi, A. Georgiadis, A. Collado, M. M. Tentzeris, IET Microw. Antenna. P 7, 858 (2013).

[11] G. Niarchos, G. Dubourg, G. Afroudakis, M. Georgopoulos, V. Tsouti, E. Makarona, V. Crnojevic-Bengin, C. Tsamis, Sensors (Basel) 17, 516 (2017).

[12] B. Yoon, I. S. Park, H. Shin, H. J. Park, C. W. Lee, J. M. Kim, Macromol. Rapid. Comm 34, 731 (2013).

[13] J. Sarfraz, A. Määttänen, P. Ihalainen, M. Keppeler, M. Lindén, J. Peltonen, Sensor Actuat B-Chem 173, 868 (2012).

[14] A. Maity, B. Ghosh, Sci. Rep 8, 16851 (2018).

[15] Y. B. Cho, S. H. Jeong, H. Chun, Y. S. Kim, Sensor Actuat B-Chem 256, 167 (2018).

[16] W. Shen, X. Zhang, Q. Huang, Q. Xu, W. Song, Nanoscale 6, 1622 (2014).

[17] X. Zhang, F. Lin, Q. Yuan, L. Zhu, C. Wang, S. Yang, Carbohyd. Polym 215, 58 (2019).

[18] K. Habiba, D. P. Bracho-Rincon, J. A. Gonzalez-Feliciano, J. C. Villalobos-Santos, V. I. Makarov, D. Ortiz, Appl. Mater. Today 1, 80 (2015).

[19] C. M. Yang, T. C. Chen, Y. C. Yang, M. Meyyappan, C. S. Lai, Sensor Actuat B-Chem 253, 77 (2017).

[20] C. Liu, H. Tai, P. Zhang, Z. Yuan, X. Du, G. Xie, Sensor Actuat B-Chem 261, 587 (2018).

[21] M. Peng, D. Lv, D. Xiong, W. Shen, W. Song, R. Tan, J. Electron. Mater 48, 2373 (2019).

[22] W. Shen, Sensor Actuat B-Chem 166, 110 (2012).

[23] S. B. Kulkarni, Y. H. Navale, S. T. Navale, F. J. Stadler, N. S. Ramgir, V. B. Patil, Sensor Actuat B-Chem 288, 279 (2019).

[24] Z. Wu, S. Zhu, X. Dong, Y. Yao, Y. Guo, S. Gu, Z. Zhou, Anal. Chim. Acta 1080, 178 (2019).

Figures

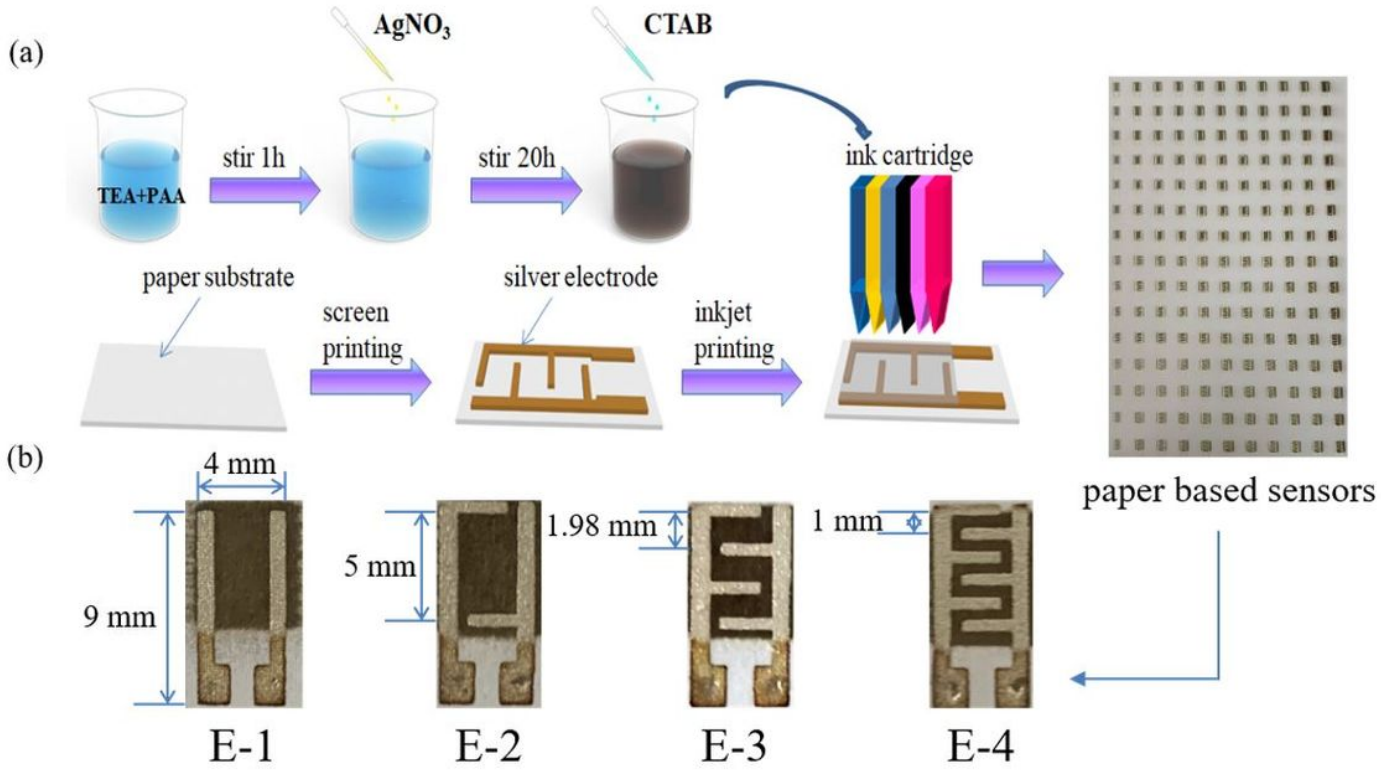

Figure 1

(a) Illustration of the fabrication process for PAA/AgNP based film sensors (b) the images of differently shaped interdigital electrodes.

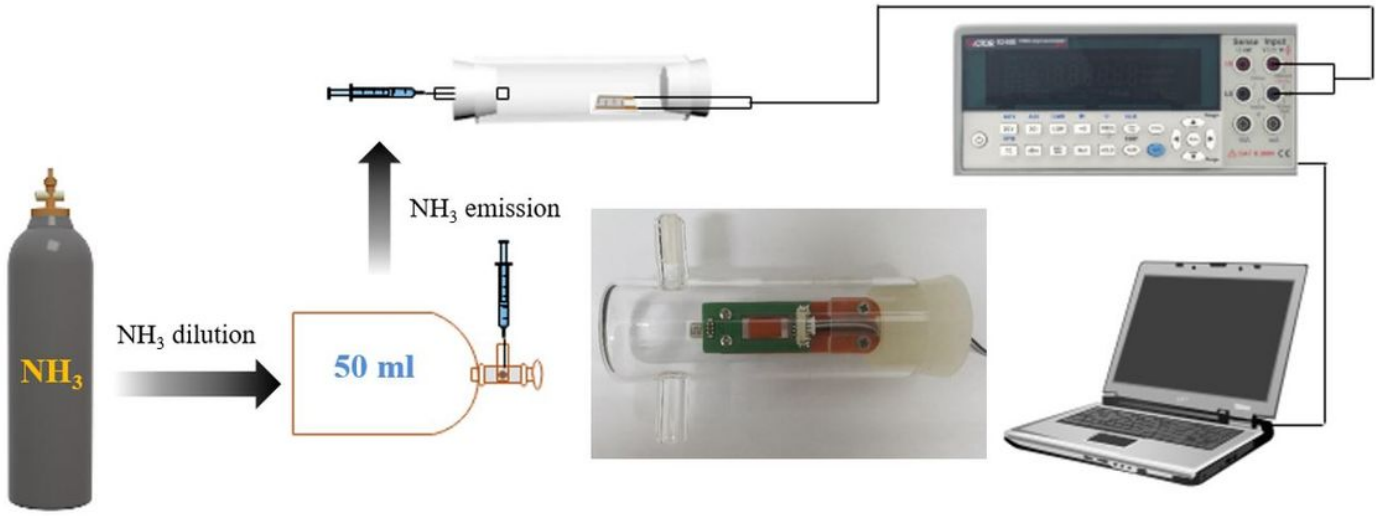

Figure 2

Schematic diagram of the gas sensing performance measuring system.

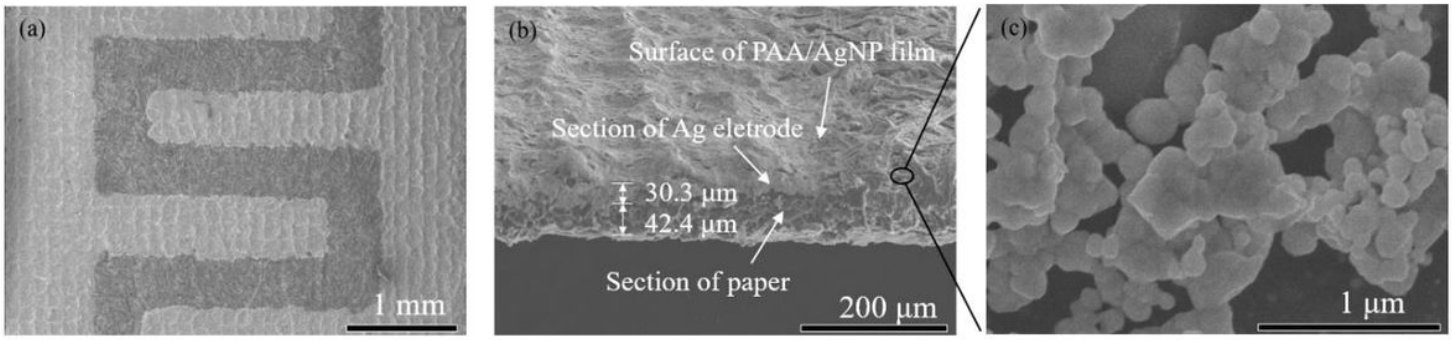

Figure 3

SEM images of PAA/AgNP film on the paper substrate with E-4 printed for 20 cycles: (a) the surface, (b) the cross-section and (c) the AgNPs coated by PAA on the paper substrate.

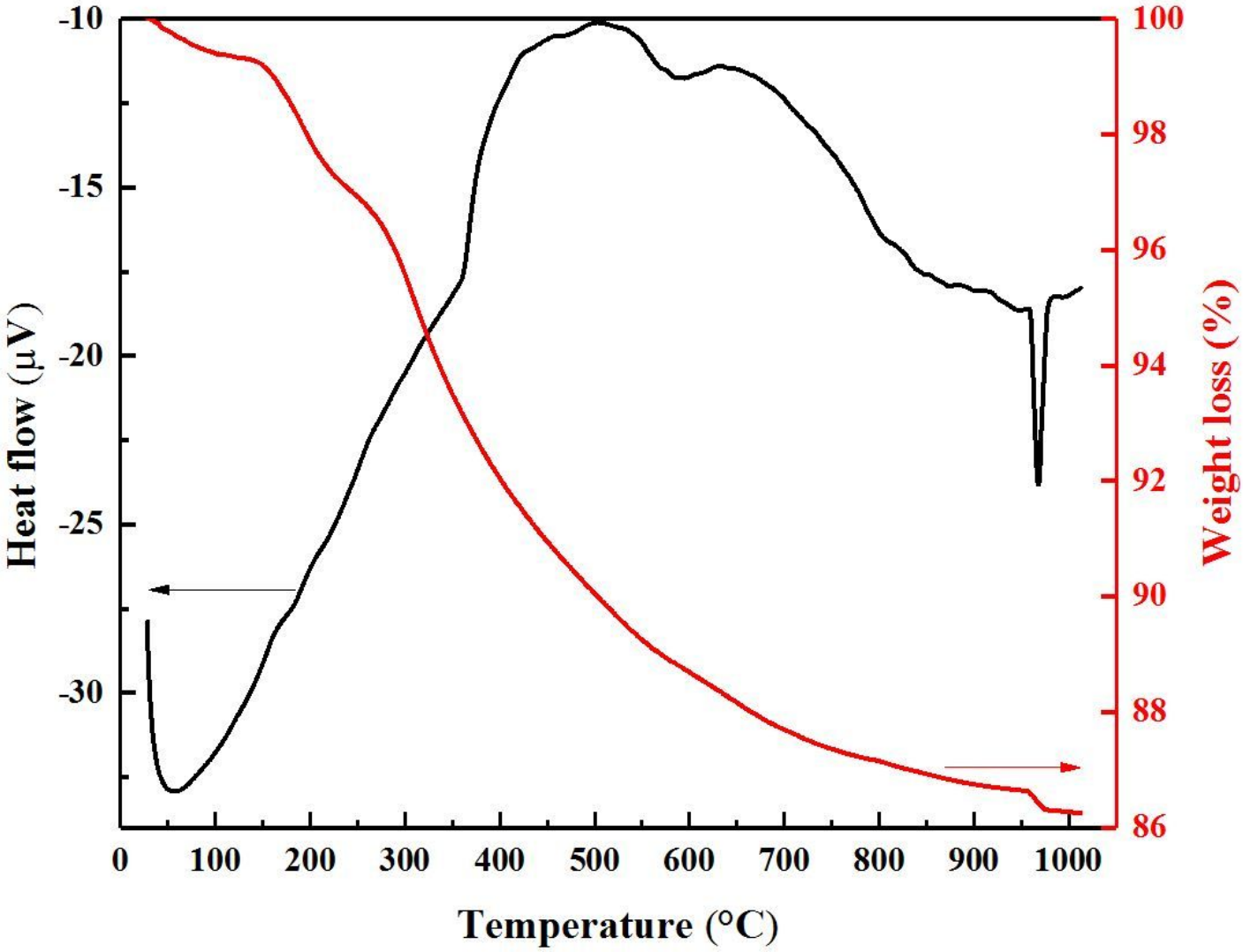

Figure 4

TG/DTA of the PAA/AgNP composite

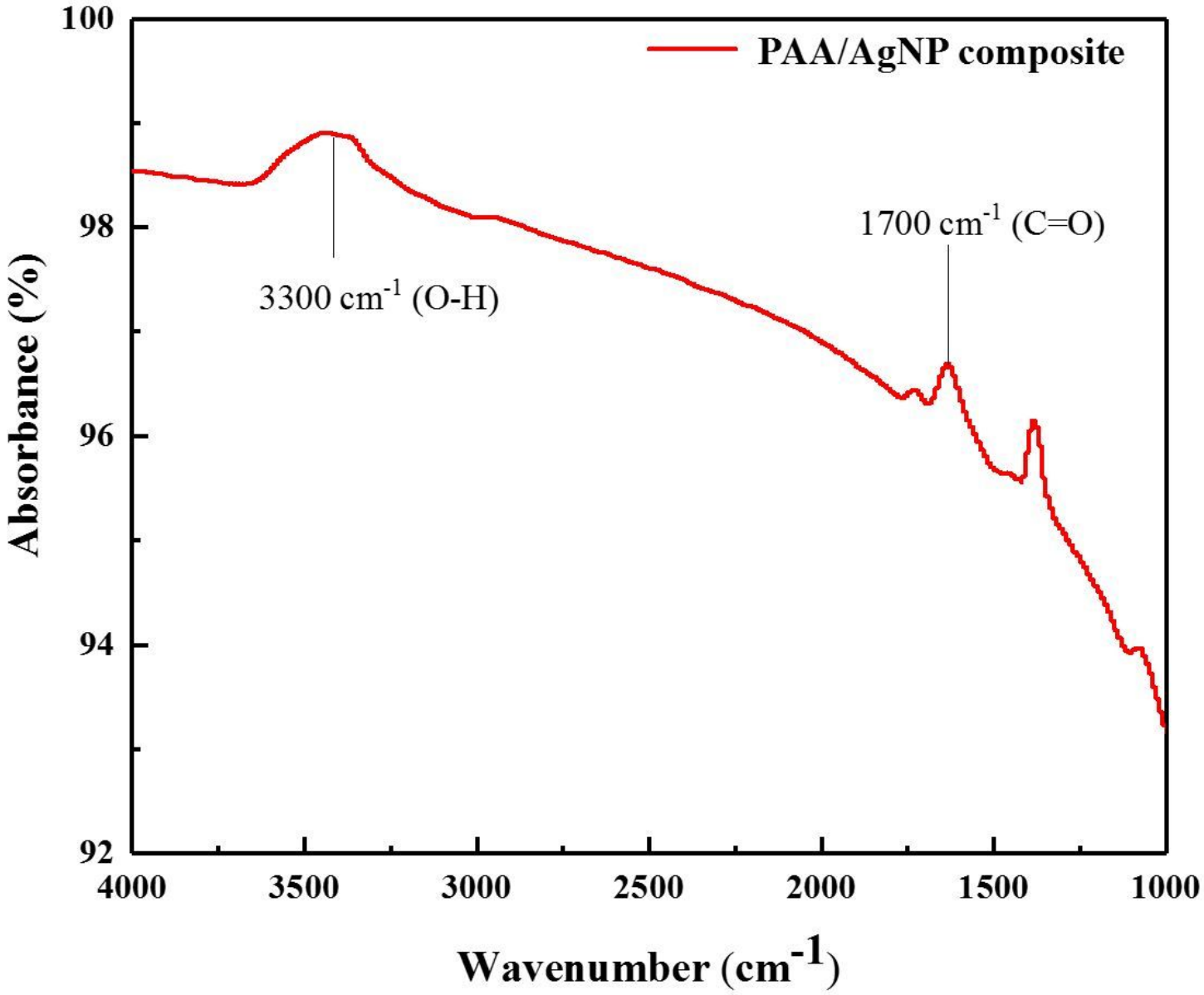

Figure 5

FTIR spectrum of the PAA/AgNP composite.

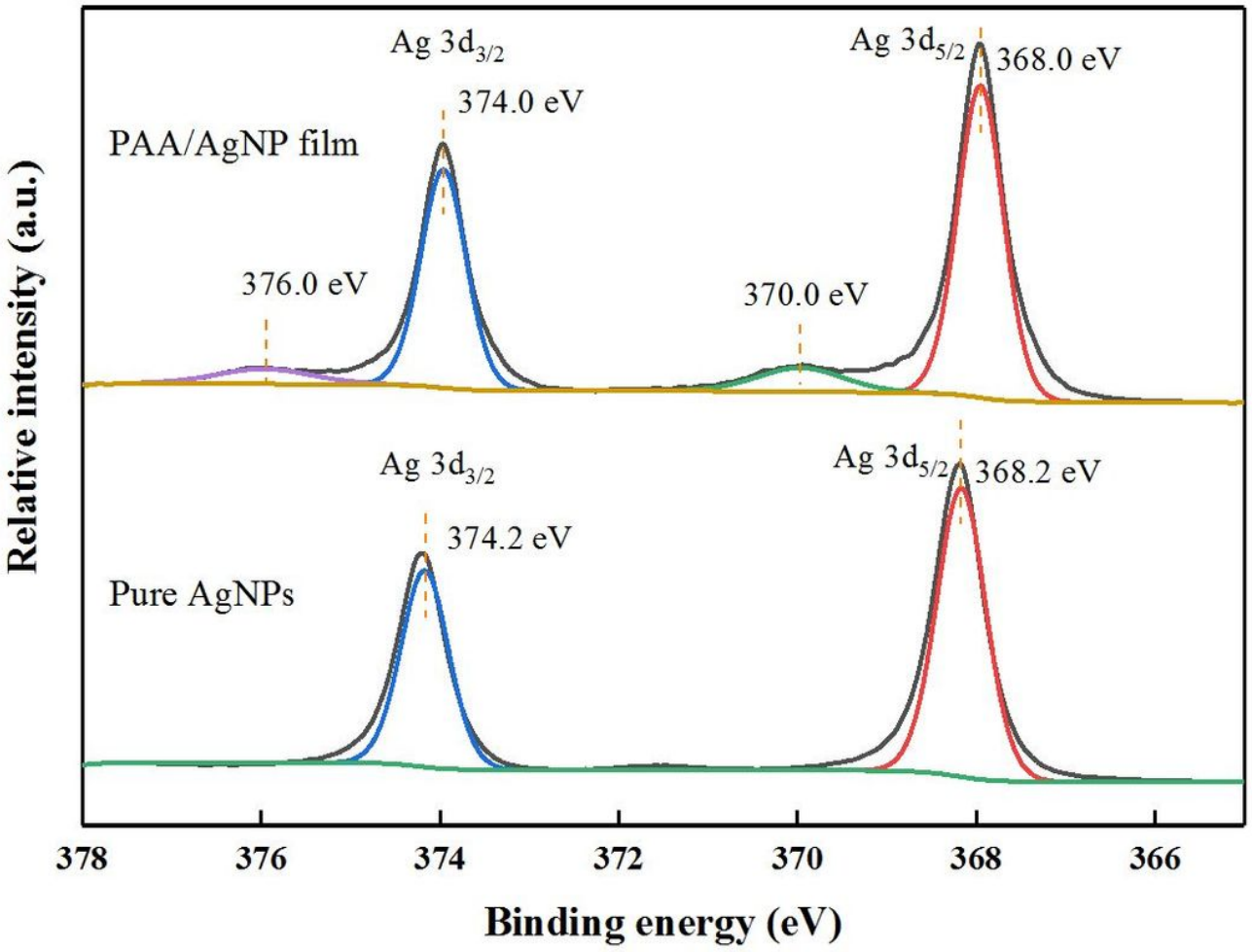

Figure 6

XPS spectra of Ag 3d in the PAA/AgNP film and pure AgNPs.

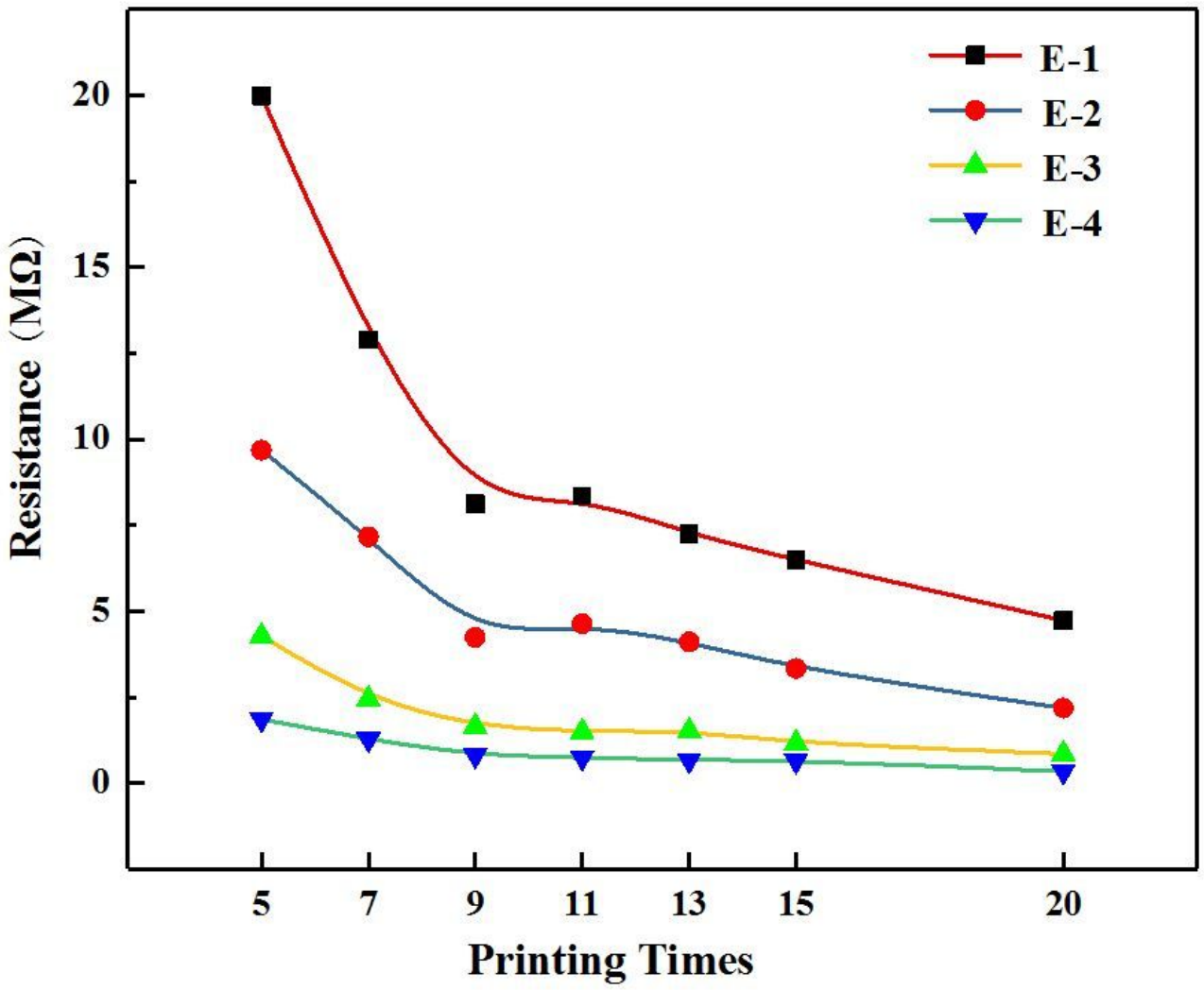

Figure 7

The relationship between the film's electrical property and thickness using differently shaped interdigital electrodes at 20°C.

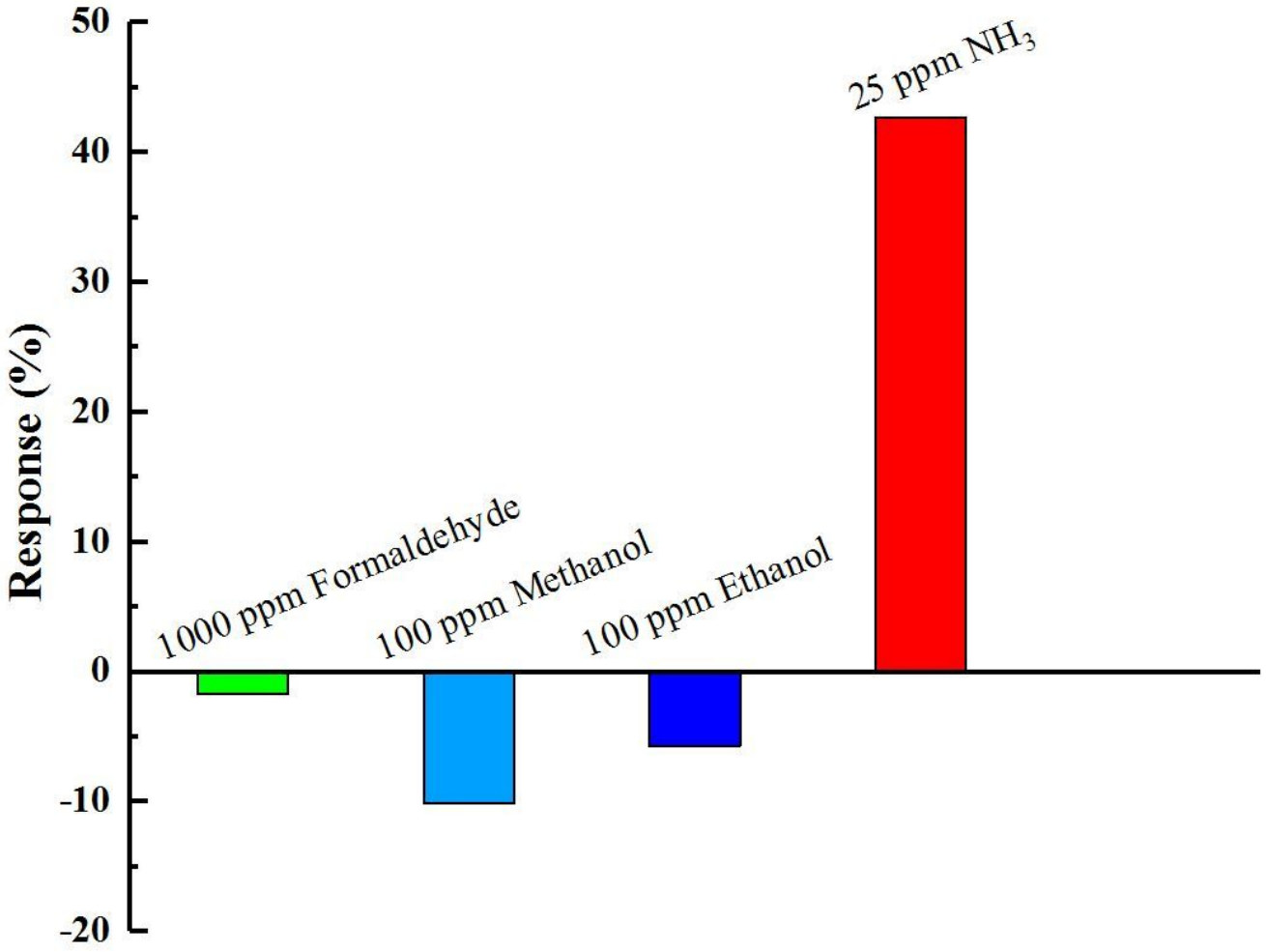

Figure 8

The responses of PAA/AgNP film sensor to four different gases at 20°C.

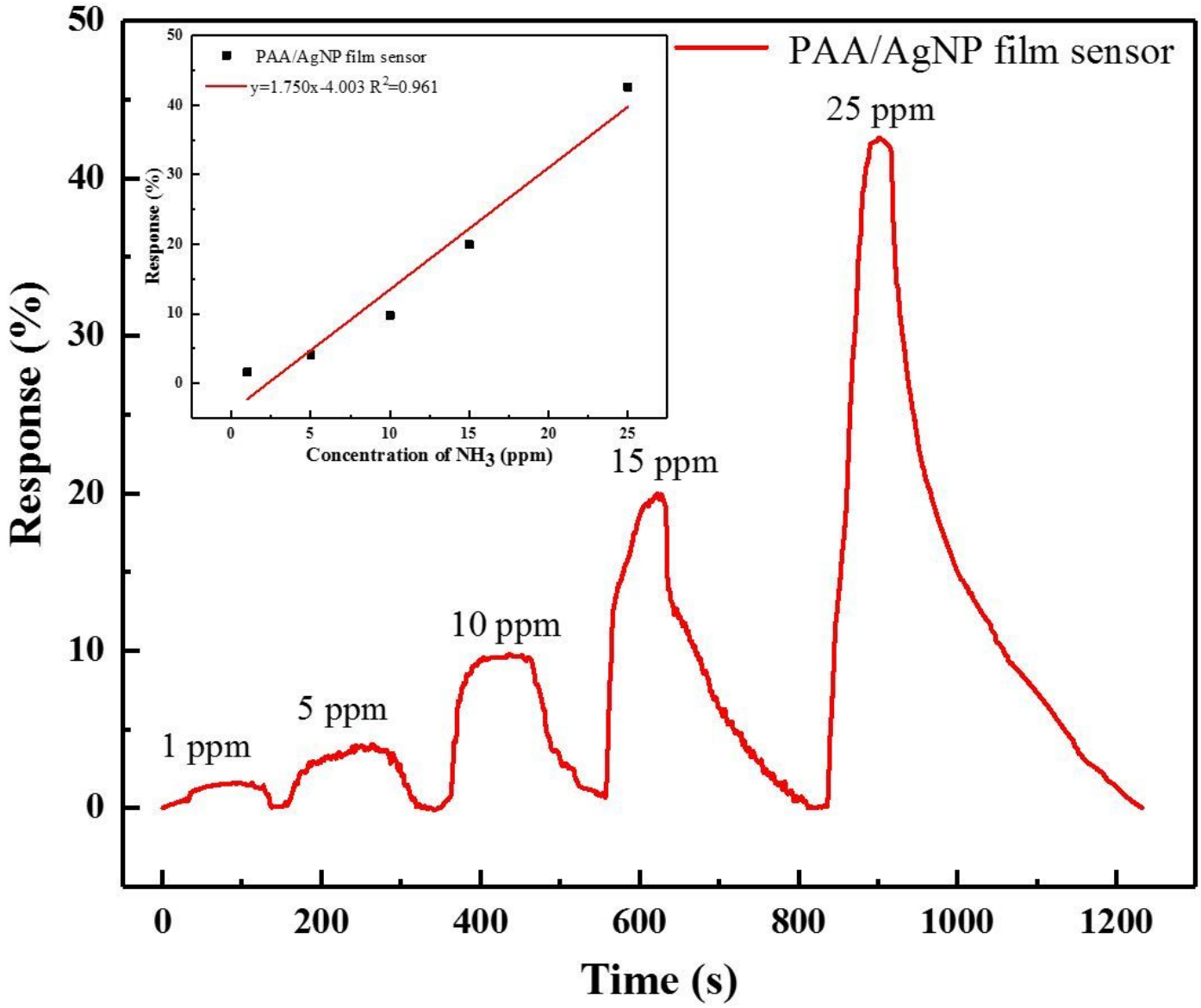

Figure 9

The response of PAA/AgNP film sensor to 1–25 ppm NH3 at 20°C (Inset figure shows a linear relationship between the response value and the NH3 concentration).

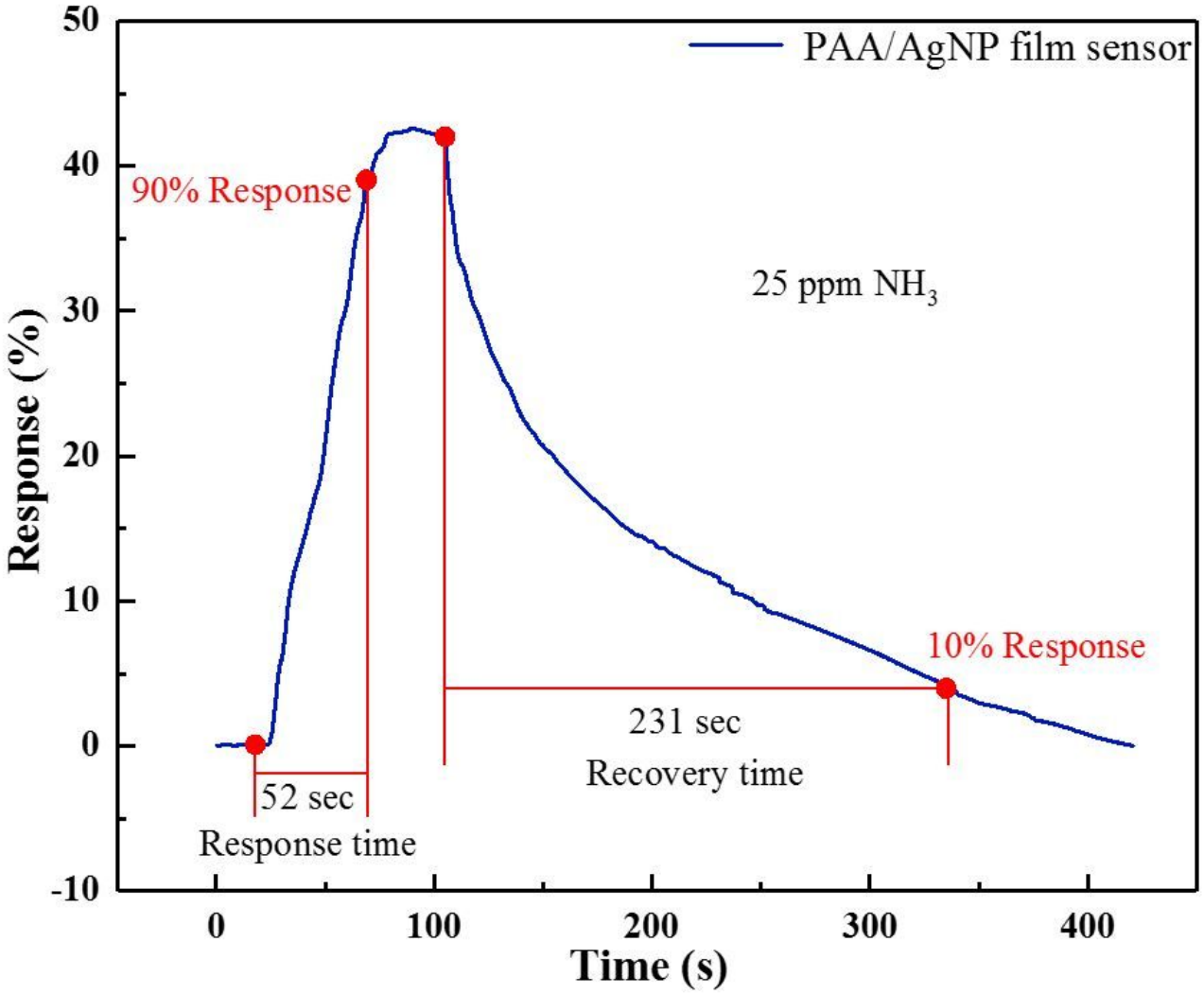

Figure 10

The response and recovery time of PAA/AgNP film sensor to 25 ppm NH3 at 20°C.

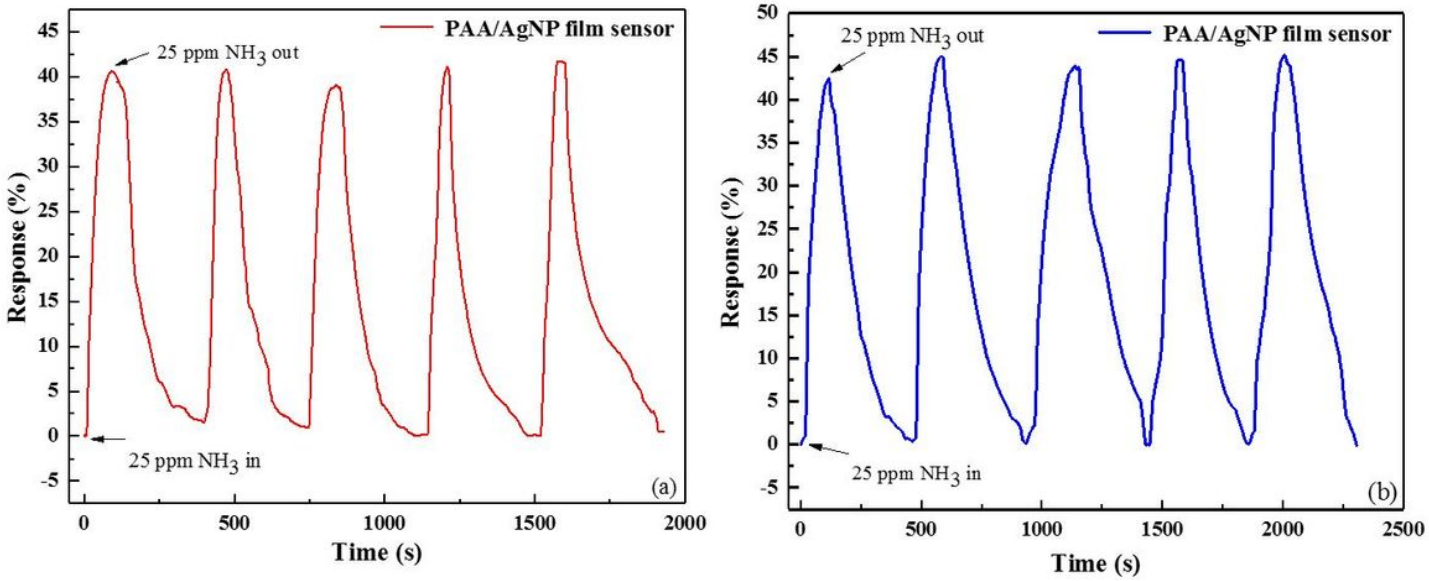

Figure 11

Test of (a) short-term repeatability and (b) long-term stability after a month of PAA/AgNP film sensor to 25 ppm NH3 at 20°C.

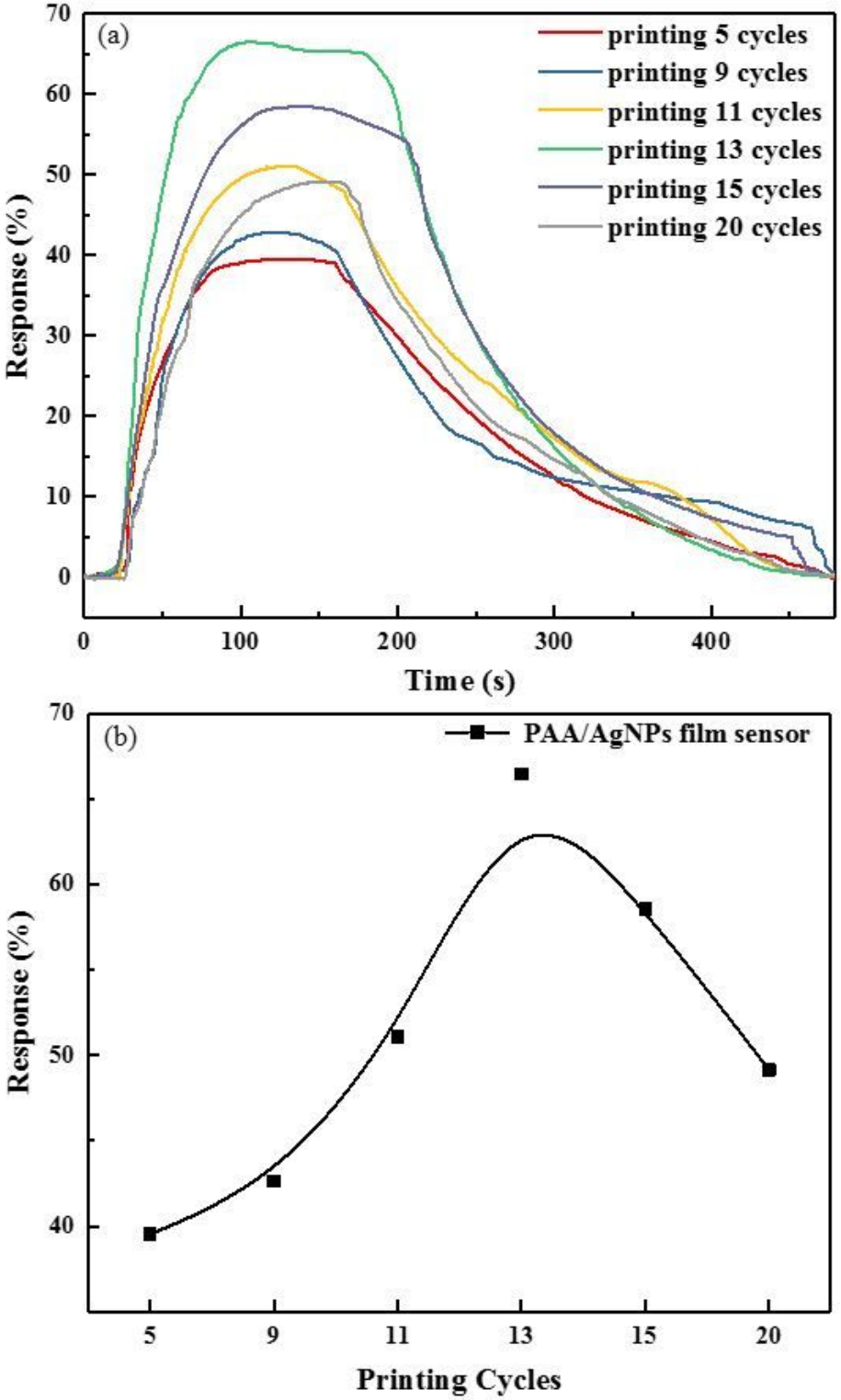

Figure 12

(a) Real-time response curves and (b) the response diagram of PAA/AgNP film sensor to 25 ppm NH3 with different printing cycles at 20°C.

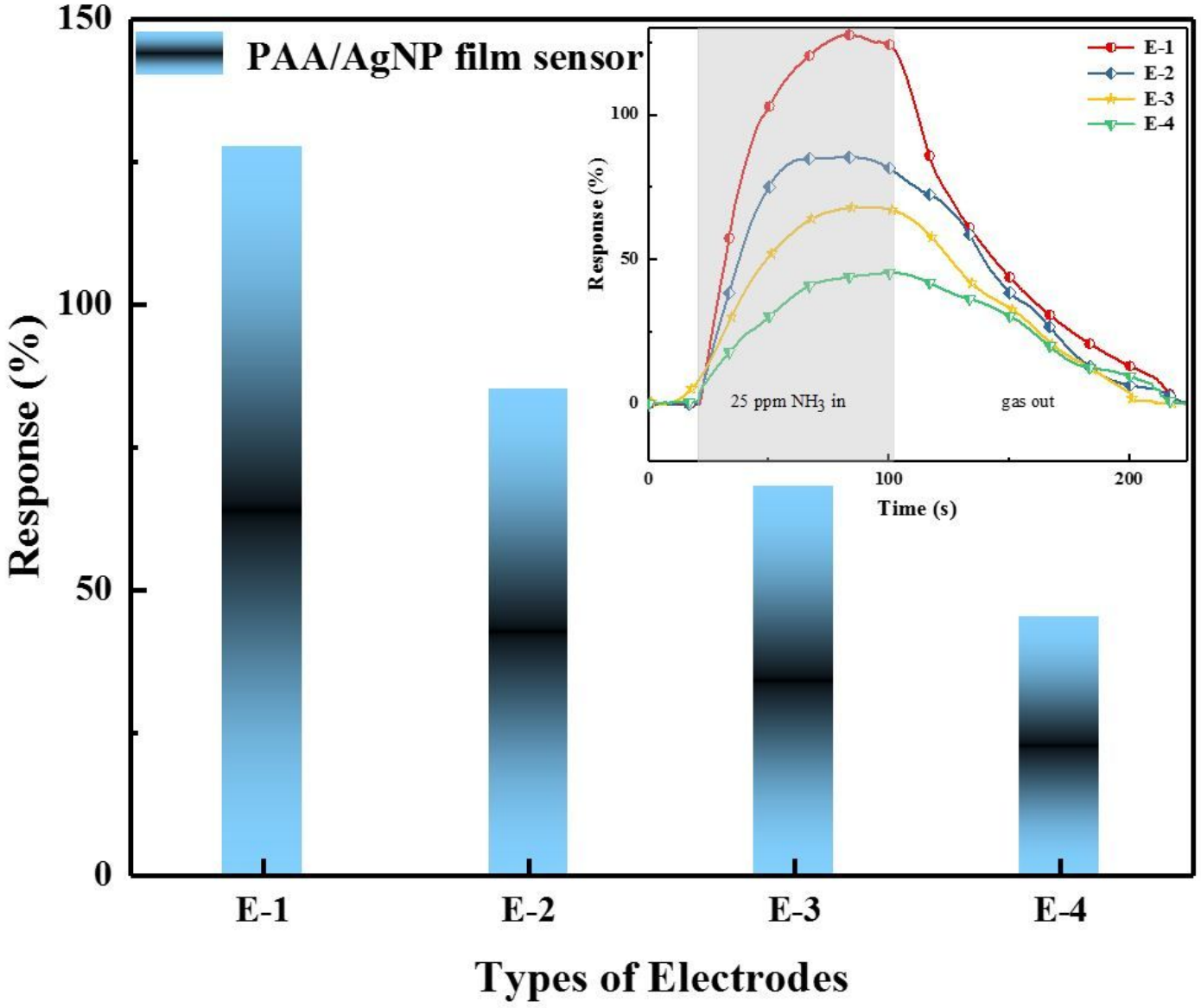

Figure 13

The responses of PAA/AgNP film sensors with different types of electrodes to 25 ppm NH3 at 20°C (Inset figure shows the dynamic response curves of four type sensors printed for 9 cycles).

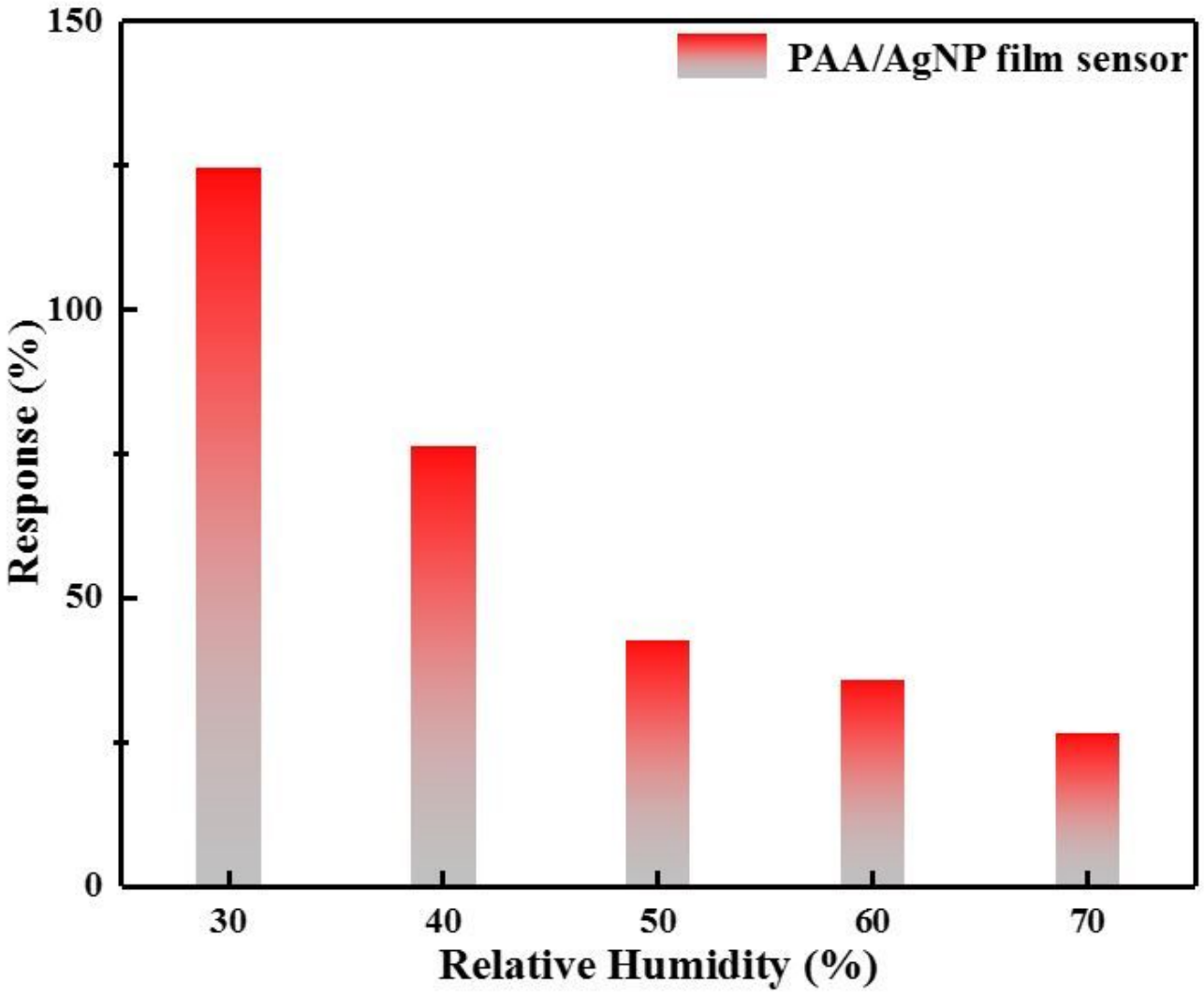

Figure 14

The influence of relative humidity on the PAA/AgNP film sensor response to 25 ppm NH3 at 20°C.

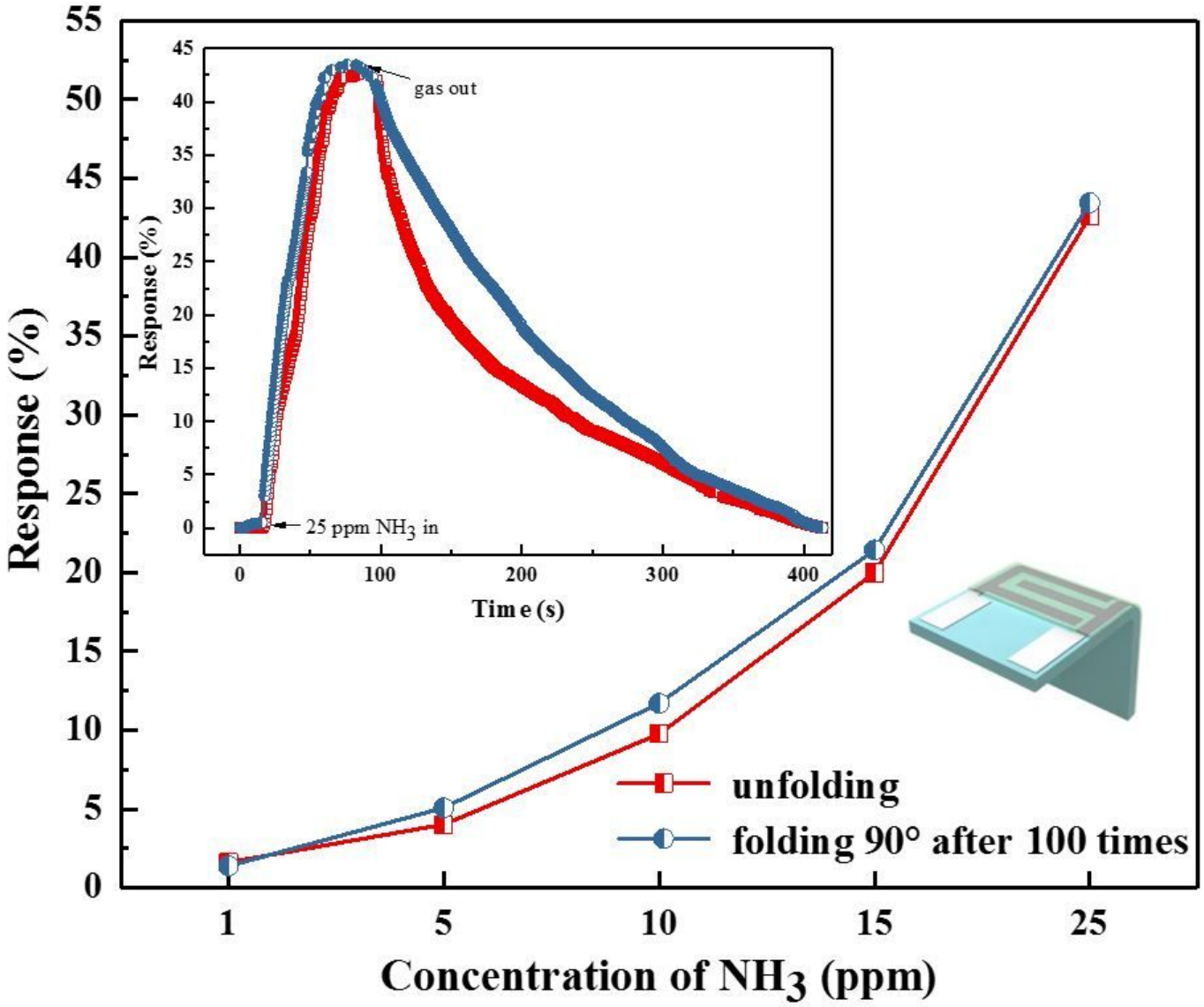

Figure 15

The influence of folding 90° after folding/ extending times on the PAA/AgNP film sensor response to 25 ppm NH3 at 20℃ (Inset figure shows the response-recovery curves of PAA/AgNP film sensor to 25 ppm NH3).

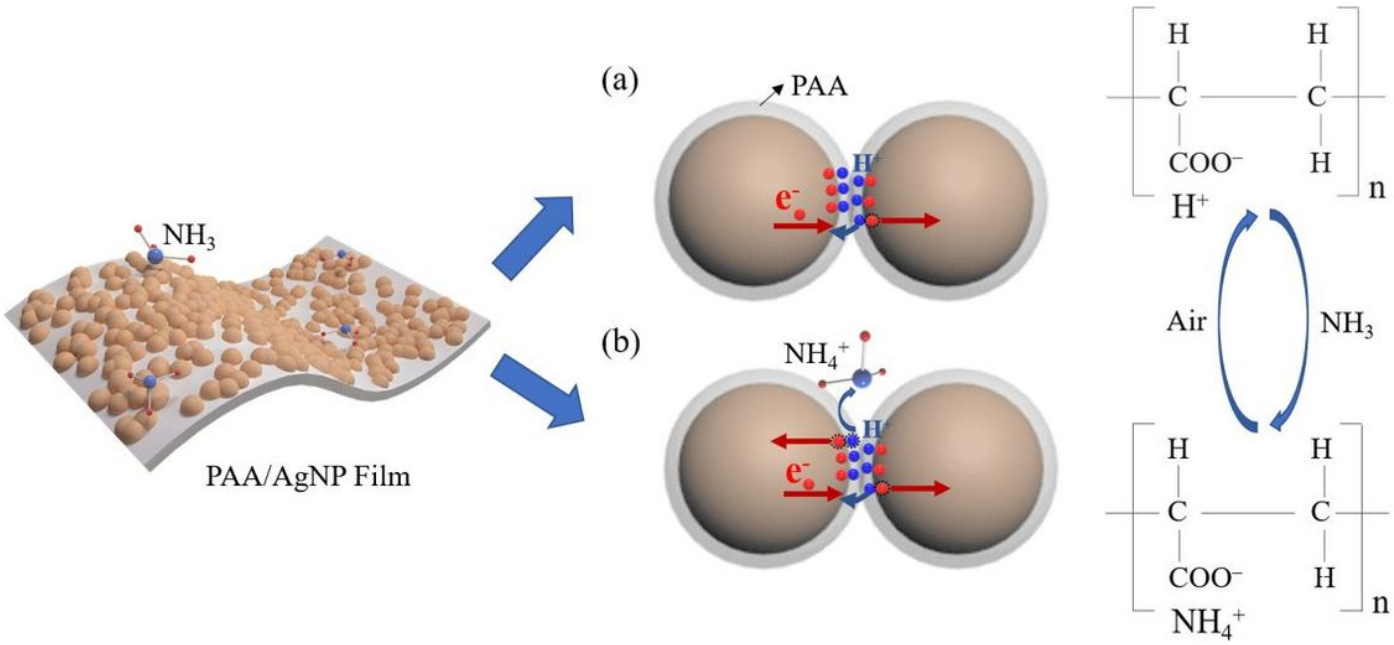

Figure 16

Schematic illustration of sensing mechanism of PAA/AgNP film sensor in (a) air and (b) NH3.

Supplementary Files

This is a list of supplementary files associated with this preprint. Click to download.

- Graphicabstract.jpg